I. INTERFERENCE DURING BURNING OF BODY-CENTERED CUBIC ARRAYS OF NINE FUEL DROPLETS IN AIR

II. SPRAY FORMATION AND EVAPORATION

Joseph Norman Kanevsky

I. INTERFERENCE DURING BURNING OF
BODY-CENTERED CUBIC ARRAYS OF
NINE FUEL DROPLETS IN AIR

II. SPRAY FORMATION AND EVAPORATION

ACKNOWLEDGMENT

The author wishes to express his appreciation to Dr. S. S. Penner, under whose direction the investigations and data reduction were carried out, for his active assistance and for suggesting this investigation. He also extends thanks to Messrs. D. Weber and A. Fuhs for invaluable assistance with the experimental work, to Betty Wood for her work on the figures, and to Helen Burrus for her typing. Support for the experimental and theoretical studies through the U. S. Army, Office of Ordnance Research, under Contract DA 04-495-Ord-446, is gratefully acknowledged.

ABSTRACT

In order to gain some understanding of interference effects during the combustion and evaporation of fuel sprays, simple three-dimensional body-centered cubic arrays of nine n-heptane or nine methyl alcohol droplets burning in air have been studied. Different cube sizes were used to vary the amount of interference obtained during combustion of the droplets. Photographic studies of the center droplet in this nine-droplet array were made in order to determine the qualitative effects of droplet spacing on the evaporation constant (K') while combustion was in progress and to determine whether the mass rate of burning was proportional to the first power of droplet diameter for a three-dimensional array of droplets.

Experimental results indicate that, when the droplets are in close proximity and the flames completely merged, the evaporation constant is reduced by 40 percent below the value obtained for minimum interference. A 25 percent increase in the evaporation constant over single-droplet values for K' was noted when the droplet spacing was altered to reduce local heat losses from the flame fronts. The results obtained from studies of the center droplet substantiate Probert's assumption (Ref. 38) that the square of droplet diameter decreases linearly with time.

Unsuccessful attempts to study the combustion of liquid bipropellant mixtures and to examine the "burning" of red fuming nitric acid in an ammonia atmosphere are described.

In Part II, a general discussion of information available on the disintegration of liquid jets, spray characteristics, mean droplet size, droplet-size distribution, and spray evaporation is presented. The use of similarity considerations in analyzing spray-nozzle performance is demonstrated. Calculation of K' for a spray from experimental spray evaporation data is described and the results of these calculations tabulated.

TABLE OF CONTENTS

LIST OF TABLES

LIST OF FIGURES

LIST OF FIGURES (cont'd)

NOMENCLATURE

D°	initial droplet diameter
D	droplet diameter at time t
$\bar{D}$	size constant in distribution laws
d	any mean droplet diameter
d'	orifice diameter
d_w	a weight mean droplet diameter
F	flow number (flow rate in gallons per hour divided by the square root of the pressure drop in psi.)
K'	evaporation constant (area per unit time)
L	a length characteristic of a spray nozzle
$M'g$	a constant, the geometric mean for mass distribution
n	distribution constant in distribution laws
p	pressure in psi
R	weight or volume fraction of the spray composed of droplets with diameters larger than D
s	spray penetration
S. M. D.	Sauter Mean Diameter
t	time in seconds
t_r	residence time in seconds
v	efflux velocity
Δp	pressure drop in psi
Γ	gamma function
μ	micron (10^{-4} cm)
μ_ℓ	absolute viscosity of the liquid

μ_m	absolute viscosity of the surrounding medium
ν_ℓ	kinematic viscosity of the liquid
ϕ, Φ, ψ, F	functional notation
ρ_a	density of the air
ρ_ℓ	density of the liquid
ρ_m	density of the surrounding medium
σ	standard deviation of droplet diameter
σ_ℓ	surface tension of the liquid
θ	spray cone angle

PART I. INTERFERENCE DURING BURNING OF BODY-CENTERED CUBIC ARRAYS OF NINE FUEL DROPLETS IN AIR

I. INTRODUCTION

The combustion of fuel sprays is of great practical importance in the construction and design of present-day propulsion equipment (Refs. 1 to 9). Although there is a wealth of experimental data (Refs. 9 to 21), no adequate theory is available to describe properly the combustion processes of clouds of droplets when subjected to various ambient conditions. On the other hand, the burning of isolated single fuel droplets in oxidizing atmospheres is relatively well understood (Refs. 22 to 37). The greatest difficulty in extrapolating the information available on single-droplet burning to spray combustion seems to be associated with the lack of information about interference effects during combustion and evaporation in sprays. Recently, some work has been done on interference effects between two and five stationary fuel droplets burning in air (Refs. 30 and 33). These studies show clearly that the square of the droplet diameter (D^2) decreases linearly with time (t). However, the slope of the D^2 vs. t curve could not be explained on the basis of any simple theory. It appears that the diffusion theory for the burning of single droplets will have to be modified in order to introduce convection effects, proper allowance for radiant heat transfer, chemical reaction rates, and for interference during burning.

Analysis of experimental data on spray combustion requires some well-defined point of departure. Some years ago, an important

theoretical study was carried out by Probert (Ref. 38). In his study, Probert assumed that the drop-size distribution was determined by the Rosin-Rammler distribution law, viz.,

$$R = \exp\left(-\frac{D}{\overline{D}}\right)^{n} \tag{1}$$

where R equals the weight or volume fraction of spray with drops of diameter greater than D, $\overline{D}$ is the "absolute size constant", n is the "distribution constant".

Subsequent to Probert's work, a similar analysis was made for other drop-size distribution laws (Ref. 39). Furthermore, it has been found that the Rosin-Rammler expression was of use over a fairly wide range of operating conditions encountered in combustion equipment utilizing fuel sprays (Refs. 40 to 43). The Rosin-Rammler distribution law is simpler to handle than two other useful equations (Ref. 40). The Nukiyama-Tanasawa equation is

$$R = 1 - \frac{\left\{\Gamma\left[\frac{D}{\overline{D}}\right]^{n}\right\}\frac{6}{n}}{\Gamma\left[\frac{6}{n}\right]} \tag{2}$$

where Γ signifies the gamma function (in the present case, the incomplete gamma function), i.e.,

$$\Gamma\left[(x)^{n}\right] = \int_{0}^{x} x^{n-1} e^{-x}\, dx. \tag{3}$$

The log probability equation has the form

$$R = \frac{1}{2} \mp \frac{\Gamma\left[\log \frac{D}{(M'g)^{1/2}}\right]}{2\Gamma\left(\frac{1}{2}\right)} \tag{4}$$

where the minus sign is used for $\log \frac{D}{M'g} > 0$ and the plus sign for $\log \frac{D}{M'g} < 0$, M'g equals the geometric mean for mass distribution, i.e., the value of D when R = 0.50, and Γ now signifies the complete gamma function,

$$\Gamma(n) = \int_0^\infty x^{n-1} e^{-x} dx = (n-1)! \qquad (5)$$

It is of interest to note that both the Rosin-Rammler and log-probability equations were developed from data for size distributions in powdered solids, whereas the Nukiyama-Tanasawa equation was derived from experimental data for air-atomizing nozzles.

Probert's second assumption was that the mass rate of burning of the droplets is proportional to the first power of droplet diameter. It is then readily shown that

$$D^2 = (D^\circ)^2 - K't \qquad (6)$$

where D is the droplet diameter at any time t, D° is the initial diameter and K', called the "evaporation constant", has dimensions of area per unit time. Probert showed how to calculate the percentage of unevaporated or unburnt fuel as a function of $\sqrt{K't_r}/\bar{D}$ for n varying from 2 to 4. Here t_r is the residence time of the droplets in the combustion chamber. Probert's theoretical curves (figure 1) show that the time for evaporation of a given quantity of fuel is more sensitive to variations in $\bar{D}$ than in n; however, n has a strong influence on the time necessary to evaporate the last few percent of the spray. A small value of n gives a small mean diameter of drop sizes in the injected spray, which indicates a high rate of evaporation. However, after burning is about three-fourths

completed, the effect of n is reversed and the rate of burning decreases for small values of n.

An attempt by Graves and Gerstein (Ref. 2) to use single droplet data for K' in spray combustion was not successful. These investigators measured combustion efficiency as a function of oxygen concentration for a single tubular combustor, using isooctane as the fuel with counter-stream injection. Observed combustion efficiencies were compared with those calculated using Probert's theoretical analysis, in conjunction with values of K' measured or calculated for the burning of single droplets. The observed data could not be completely explained unless spray combustion involves effects, at least for over-all oxygen concentrations below 24 percent, which can be ignored in the burning of single droplets.

The earlier experimental efforts to test the validity of equation 6 for single-, two-, and five-droplet arrays (Refs. 30 to 35) indicated that, for steady burning in an oxidizing atmosphere, K' was constant over the range of drop sizes tested. Since equation 6 is believed to correlate all observed results for combustion of single fuel droplets in an oxidizing atmosphere and apparently holds also for simple planar arrays of droplets, it seemed desirable to check the validity of the functional form of this equation also for a three-dimensional array. As a simple example of a three-dimensional array, a body-centered cubic spatial arrangement was chosen with droplets at the eight corners of the cube and the droplet to be studied located at the center of the cube. Since any finite spray can be approximated as a superposition of simpler three-dimensional arrays, studies of the burning law for a body-centered cubic

lattice should shed some light on the validity or failure of equation 6 to represent a phenomenologically acceptable description of burning rate. Also, the use of a small number of drops which can be closely scrutinized may provide some clues for the important physico-chemical processes operative during droplet burning. Therefore, experiments were carried out to determine if equation 6 holds for a three-dimensional array and, if so, to find K' for the body-centered cubic array as a function of drop-spacing. Cube sizes were selected so that flame shapes for the array varied from separated flame fronts for each droplet, to partially merged flame fronts, and finally to completely merged flames with a single flame envelope.

A summary of the experimental procedure and results is presented in Sections II and III of Part I for n-heptane and methyl alcohol droplets burning in air.

Unsuccessful attempts at using the experimental techniques described above for the study of liquid bipropellant mixtures and for the "burning" of red fuming nitric acid in an ammonia atmosphere will be described in Section IV of Part I.

II. EXPERIMENTAL PROCEDURE

All of the experimental data were derived from motion picture studies and measurements of droplets suspended by means of quartz fibers properly mounted in a body-centered cubic array. The desired geometric spacing of the fibers was obtained by cementing the fibers to supports attached to metal rods. The rods, in turn, were supported by clamps fastened to a suitable stand. The arrangement of the fibers with the desired spacing presented some difficulties in that the Sauereisen cement used had a tendency to shrink when drying. This shrinking produced a change in the arrangement of the fibers. Two methods were used to avoid this difficulty. These are: (1) the fibers were mounted in groups of four by using two parallel metal plates with holes drilled at the desired spacing or (2) the fibers were cemented to individual soft copper wires which could be bent to yield any desired spacing. The latter method is simpler to use but does not provide a completely rigid support for the fibers. In practice, a combination of these two methods was employed. The pairs of four fibers, attached to each of two bars, were arranged at angles of 15 to 45 degrees from the horizontal; the fibers supported from the bars provided the cubic arrangement desired when the bars were brought together within the prescribed distance (figure 2). The center droplet was supported separately from another bar.

The fuel was placed on the droplets by use of a hypodermic syringe and needle. As can be seen in figure 3, the droplets were reasonably spherical. It was possible to ignite the droplets with a match.

The burning droplets were photographed by use of an electrically-driven Arriflex 35 mm movie camera. Back lighting was provided by a 100 watt bulb located about seven inches away from the droplets. A telephoto lens was used with a ten inch adapter tube in order to obtain as large an image as possible. The film gave images of nearly the actual size. The high magnification reduced the depth of field to the order of a droplet diameter. However, only the center droplet was of interest in the present experiments; the corner droplets closest to the camera lens were slightly out of focus and the rear corner droplets were, in most cases, not visible because the camera was mounted almost directly in front of one face of the cube.

Kodak Plus-X film was used for drop-size measurements, whereas Kodak Tri-X was employed to photograph the flame front and shape.

A stroboscope served as a timing standard. A ten-inch circular aluminum plate, with three holes 120 degrees apart near the periphery, was secured to a 75 r.p.m. constant speed motor giving 3.75 flashes per second. The stroboscope was placed directly behind the burning drops. The camera speed was adjusted to the maximum of about 25 frames per second.

Calibration of drop diameter was obtained by photographing a 3/32 inch ball bearing for each 100 feet of film. This ball bearing was photographed under the same conditions as were used for the center droplet.

The film was measured by use of a microfilm recorder and a millimeter scale. Two measurements were made on each drop, i.e., the two perpendicular diameters inclined 45 degrees to the major and

minor axes in the plane of observation. The arithmetic mean value of these two readings was recorded as the "effective diameter" of the droplet. It is readily shown that the volume of a sphere with the measured "effective diameter" is not very different from that for the prolate spheroid shape assumed by the droplet under gravitational and surface tension forces. The use of the microfilm recorder provided a magnification of about 35 diameters. Measurements were made every third to seventh frame from ignition to the point where any one of the droplets under study was completely burned out.

In order to obtain a complete picture of the lower flame shape for conditions varying from little interference to complete merging of the flame for all the droplets, a shorter adapter tube was used with the same telephoto lens on the camera. Representative photographs of this type are shown in figure 4.

III. EXPERIMENTAL RESULTS

Values of K', the evaporation constant, were calculated by determining the slope of the D^2 vs. t curves for the center droplet in each experiment. These results are listed in Tables I and II for n-heptane and methyl alcohol, respectively. In Table III, average values of K' are shown for the two fuels for all spacings. Representative curves for several runs are plotted in figures 5 to 10. The data plotted in figures 5 to 10 indicate that D^2 was a linear function of time, t, (within the limits of experimental accuracy) for the center droplet. Several of the runs showed a low-frequency, small-amplitude, oscillation for D^2 about the values falling on the "best" straight line. This oscillation was probably produced by mechanical vibrations of the quartz fibers. Slight spurious vibrations in the supports introduced an oscillation of the fibers which, in turn, caused the droplets to move. Since the camera shutter was at a fixed speed and the rate of film transport was 25 frames per second, the movement of the droplet could cause a slight distortion of the image on the film, which might possibly manifest itself as a variation in measured drop diameter.

In the paper by Goldsmith and Penner (Ref. 31), the results of the calculation of K' from the theory derived for the simple model of steady burning are tabulated for several fuels including n-heptane. In Table IV are listed the values of K' obtained for single droplets from this theory and from Godsave's experiments (Ref. 35), as well as the values for two-, five-, and nine-droplet arrays.

As is readily apparent from the data shown in figures 11 and 12 and listed in Tables I and II, the extent of interference between droplets

has a significant effect on the evaporation constant. For the case in which the droplets are in close proximity and the flames are completely merged (see figure 4), K' was reduced by 40 percent below the value obtained for minimum interference. This reduction provides positive evidence for the practical importance of locally fuel-rich zones on burning rates. Oxygen deficiency for interfering droplets is undoubtedly responsible for the observed decrease in evaporation constant. In figure 13, data are presented from the paper by Rex, Fuhs, and Penner (Ref. 30) for the variation in K' with spacing for two droplets of n-heptane. Spacings for the nine-droplet three-dimensional array were not varied over wide ranges and, therefore, the shape of the K' vs. spacing curve obtained from nine-droplet data (figures 11 and 12) cannot be positively established. However, the results suggest qualitatively that, depending on droplet spacing, the effective value of K' may be equal to, less than, or greater than the value of K' which is appropriate for a single isolated fuel droplet.

The present results have led to the following practically important conclusions:

(1) The droplet burning relation

$$D^2 = (D^\circ)^2 - K't \qquad (7)$$

holds not only for one-, two-, and five-droplet arrays, but also for a three-dimensional nine-droplet array. Therefore, it seems likely that it applies also to sprays, and that equation 6 forms an acceptable postulate for a phenomenological analysis of spray combustion.

(2) Spray design may have a profound effect on the effective burning rate by reducing K' significantly in locally fuel-rich environments.

(3) The enhancement in burning rate over the single droplet results, which can be produced through optimum spray design, should be at least as large as 25 percent, the greatest increase observed in the present investigations. For poor spray design, the evaporation constant can be reduced easily by as much as 40 percent, which is the largest reduction observed in the burning of nine-droplet arrays.

IV. UNSUCCESSFUL ATTEMPTS AT BURNING VARIOUS FUEL-OXIDIZER COMBINATIONS

The objective of the present investigations was to study the validity of the burning rate law (equation 6) for fuel-oxidizer systems of the type used in rocket engines. In particular, it was desired to see if a gaseous fuel with a liquid oxidizer would provide the same type of results as have been observed for hydrocarbon and alcohol droplets in air. An effort was made to "burn" red fuming nitric acid in an ammonia atmosphere. The attempt was made in a sealed plexiglass dry-box which had first been purged with high-purity dry nitrogen gas and then filled with NH_3 gas. The NH_3 gas was supplied continuously with a very slight positive pressure to insure a nearly uniform atmosphere in the dry-box. However, efforts to obtain a droplet of RFNA on a quartz fiber in the chamber resulted only in the immediate formation of ammonium nitrate at the surface of the RFNA droplet. The spark ignition source could not be used successfully and a heterogeneous diffusion flame could not be established.

Because liquid bipropellant fuels are customarily used in many conventional rockets, it was decided to attempt burning RFNA and aniline droplets in close proximity in an inert atmosphere. The arrangement was similar to that described above, using nitrogen as the inert gas. Again the spark ignition source, which supplied only about 20,000 volts, could not be used to ignite two-and five-droplet arrays, even when the droplet surfaces were almost touching. An effort was made to ignite the droplets by bringing them into actual contact while they were exposed to the spark ignition source. This scheme was also unsuccessful and led

only to the formation of a carbonaceous residue. A similar experiment, in which about 25 to 30 percent by weight of furfuryl alcohol had been added to the aniline, also failed to lead to a stable heterogeneous diffusion flame. Finally, a stream of RFNA was sprayed on the bottom of the chamber (covered with stainless steel) so as to intercept a stream of aniline containing furfuryl alcohol. After about one quarter cm^3 of each had been injected and a carbonaceous lump formed (similar to the residue produced when the two droplets were brought in contact), the junction of the sprays and the carbonaceous lump began to glow incandescently and finally burst into flames. This experiment verifies the well-known fact that, if sufficient concentrations of fuel and oxidizer are maintained and heat transfer from the contact area is limited, the mixture will ignite spontaneously.

On the basis of the results discussed above, it is felt that the combustion of liquid bipropellants of the type used does not lead to stable heterogeneous diffusion flames and, therefore, equation 6 probably does not provide an acceptable phenomenological description for these propellant systems.

V. DISCUSSION

The studies on two-droplet interference effects (Refs. 30, 33) showed that the value of the evaporation constant (K') was a function of the initial droplet diameters and of the spacing. No attempt was made in the present investigations to obtain detailed quantitative information on the dependence of K' on geometric parameters. Rather, the purposes of this study were (a) to verify the validity of equation 6 and (b) to show that the geometric design of the nine-droplet arrays does affect qualitatively the observed values of K'.

From studies on two droplets burning in close proximity (Refs. 30, 33), it appeared that K' was decreased in oxygen-deficient atmospheres but tended to increase when heat losses from the flame surface to the outside were minimized.

For the three-dimensional array of nine droplets, the droplet spacing enters as an indirect measurement of the interference obtained and flame shape developed. As is clearly shown in figure 4, the flame shape changes radically as the spacing is varied. Average values of K' for the three arrangements are included with the photographs shown in figure 4 and are listed also in Table III. The change in K' observed in going from the completely separated flames to the partially merged flame is too small to permit any definite conclusions. However, the reduction in evaporation constant for extensive interference between flames provides graphic evidence of the change resulting from local oxygen deficiency. Because changes in K' for the unmerged and partially merged flames were not large in comparison with the changes found for two droplets, proof of a rise in evaporation constant associated with

the reduction in local heat losses from the flame fronts is less evident. The reality of this effect is, however, suggested by the fact that K' in nine-droplet experiments exceeds by about 25 percent the single droplet values (Refs. 32, 34, 35).

Experimental data showing the reduction in combustion rate for excessively rich mixtures (Refs. 3 to 5) seems to validate the theory that mass evaporation rates and, consequently, combustion rates will be reduced when the mass concentrations of droplets per unit volume in a combustor are excessive.

Use of the information regarding the possible increase in combustion rate and K' with optimum droplet spacing may make it possible in the future to optimize spray characteristics by increasing the efficiency of combustion equipment. The success of this method of approach depends on the availability of information on evaporation constants for the various fuels and some definite knowledge concerning the atomizing characteristics of the fuel injectors used. The problem of spray formation and drop-size distribution is considered in greater detail in Part II of this thesis.

PART II. SPRAY FORMATION AND EVAPORATION

I. INTRODUCTION

It is the purpose of the present discussion to summarize critically the information available on spray formation and evaporation. Many writers have attempted to explain the factors influencing drop-size distribution and spreading of sprays from fuel nozzles (Refs. 13 to 17, 38 to 45). An extensive bibliography is provided in reference 46. Experimental studies of sprays indicate that the most important factors affecting spray distribution and atomization are the following: (1) the construction of the nozzle and associated supply equipment; (2) the physical properties of the fuel, such as density, viscosity, surface tension, etc.; (3) the physical properties of the medium into which the fuel is being discharged (Ref. 6).

Liquid fuel is usually supplied to a combustor through a fuel nozzle. The nozzle delivers the fuel to the burner or combustion chamber in such a state that vaporization and combustion will be very rapid. The transition from an initially continuous liquid jet to a vapor, or to a great number of finely divided droplets, requires the addition of energy to the fuel. The energy may be added by: (a) pressurizing the fuel chamber and subsequently converting the pressure head into kinetic energy in the nozzle; (b) the addition of heat; (c) the use of a secondary fluid, such as air, to assist in the break-up of the liquid; or (d) the use of moving parts, such as a mechanically driven spinner.

Giffen and Muraszew (Ref. 6) have recently summarized the available information on atomization of liquid fuels. The present discussion on the disintegration of liquid jets is based on the discussion given in their book.

II. DISINTEGRATION OF LIQUID JETS

The complex interaction of physical properties involved in the disintegration of liquid jets makes it difficult to correlate properly the effects of the fundamental physical factors present in the atomization process. Investigators differ greatly in the importance they attach to the various factors involved in spray formation. Thus, different parameters are used for correlating spray performance with the injection variables. In the following discussion, a qualitative outline of the probable mechanism of jet disintegration will be given.

A low-velocity liquid jet discharged through an orifice is primarily affected by gravity and surface tension forces. As the discharge velocity is increased, the liquid assumes the form of a continuous jet. Surface tension forces and disturbances in the liquid may cause the jet to collapse if its length is greater than its circumference. Such a collapse results in the formation of small drops. Strictly speaking, this critical length to circumference ratio, the importance of which was first recognized by Rayleigh (Ref. 47), applies only to non-viscous liquids. Viscous forces increase the ratio slightly. The disintegration process becomes more complicated as the primary disturbances in the liquid flow increase. These disturbances can be introduced by the atomizer, the liquid, or the surrounding medium and, in practice, are always present. In addition, these random disturbances cause vibrations at the liquid-air interfaces of the jet. The cross-section of the jet then becomes deformed in such a way that successive deformations are displaced by 90 degrees. If the wavelength of the oscillations is greater than the circumference of the jet, then surface tension forces contribute

to further deformation and subsequent disruption of the jet. Haenlein (Ref. 48) found that the optimum wavelength for jet disruption was 4.42 times the jet diameter for liquids of low viscosity and greater for very viscous liquids. As the jet velocity is increased further, the effect of the resistance of the surrounding medium becomes significant. This resistance tends to increase deformation of the jet and to reduce the critical value of the wavelength of the oscillations above which jet disintegration begins. Using air as the medium, Weber (Ref. 49) found the optimum wavelength to be 2.8 times the jet diameter for a medium-velocity liquid jet. A further increase in efflux velocity causes the jet to oscillate with respect to its axis while the cross section remains essentially constant.

Air resistance tends to increase the amplitude of jet oscillations and leads to final disruption of the jet. The wave action described above is more pronounced for viscous liquids, but viscous forces permit larger oscillations before the break-up takes place. Generally, viscous effects decrease the break-up rate of the distortions in the jet and, after break-up, tend to increase the final mean droplet size. Surface tension acts in two ways. Initially, it opposes the development of surface distortions into ligaments and droplets; however, it aids the final stages of disruption. In practice, the initial stages are of greatest importance in spray formation.

In the terminal stages of atomization of a high-velocity fluid jet, the process which is of greatest practical interest in combustion applications, the jet becomes sub-divided into many small droplets in a cone-shaped spray. Photographic studies indicate that atomization

begins immediately at the orifice, although the total mass rate of evaporation increases as finer droplets are formed. The spray is initially divided into large droplets and, as it travels down the combustor, tends to break up into smaller droplets (Ref. 44). Disintegration of a liquid jet ceases when the velocity of the liquid particles falls below a critical value for the liquid.

Disintegration of a liquid jet is promoted by turbulence in the flow of the liquid from the orifice and by the influence of turbulence in the surrounding medium. Turbulence in the flow depends on atomizer design and flow velocity. Turbulent flow is characterized by radial velocities which induce widening of the jet and final break-up. The magnitude of the resistance of the surrounding medium will be proportional to the momentum difference between the fluid jet and the surrounding medium. This difference will increase in combustion chambers where high temperatures and related higher viscosities exist.

The description given above for the break-up of a fluid jet applies to simple orifice injectors. In practical applications, the atomization process is improved by introducing greater disrupting forces such as impinging fluid streams, high centrifugal velocities, etc.

III. SPRAY CHARACTERISTICS

The spray characteristics may be discussed in terms of appearance, penetration, cone angle, dispersion, mean droplet size, spray uniformity and droplet-size distribution.

A. Spray Appearance

The spray generally appears at the atomizer tip as a cone. For simple orifice atomizers, this cone has an included angle of only a few degrees; with swirl or poppet valve atomizers, the cone is hollow and has a wide angle. In practice, the included angle is of the order of 80 degrees. Rupe (Ref. 44) suggested that the cone angle be defined as the angle in which 80 percent of the spray by weight is included. Any desired configuration of the spray can be realized through proper design of the outlet orifice and supply conditions. A finite distance from the orifice face, the spray is usually enveloped in a mist of small droplets suspended in, or moving with, the surrounding medium. The number of suspended droplets increases with increasing injection pressure or increasing density of the surrounding medium. The main spray travels inside the misty envelope. The characteristics and dimensions of the combustion chamber will usually dictate the choice of a particular spray.

B. Spray Penetration

The penetration of a spray is usually much greater than that of a single droplet injected under similar conditions since the liquid jet imparts some of its energy to the surrounding medium and thus decreases the velocity differential between the droplets and the medium. Spray penetration for continuous spray nozzles depends on the following: (a) discharge velocity, (b) properties of the surrounding medium, (c)

atomizer design, and (d) fuel properties. Secondary effects on penetration are those introduced by the degree of spray dispersion and the degree of atomization. The effect of injection pressure on penetration is not easily defined. An increase in injection pressure not only causes an increase in spray velocity but also causes an increase in the number of droplets, thereby increasing air resistance. The available experimental evidence seems to indicate that spray penetration increases with increasing injection pressure.

An increase in the density of the surrounding medium generally tends to reduce spray velocity and penetration. It is usually assumed that penetration is a function of gas density and independent of gas viscosity. The latter assumption has been shown to be true as long as the flow around the droplets is turbulent. Obviously, the atomizer design has a great effect on penetration. Probably the most important feature of the atomizer is the size of the discharge orifice. Increasing the size of the orifice leads to an increase in spray momentum with respect to the surrounding medium and, consequently, increases penetration. Counter-stream injection generally reduces penetration but improves atomization. An increase in fuel density or viscosity tends to increase penetration.

An effort has been made by Mehlig (Ref. 50) and Schweitzer (Ref. 51) to correlate the effects of different variables, such as air density, injection pressure, and orifice size with penetration. The simple relationships developed are of value in comparing the penetration of two similar sprays under various conditions. Schweitzer found

that

$$\frac{s}{d'}(1+\rho_a) = \phi\left(\frac{t\rho_a\sqrt{p}}{d}\right) \qquad (8)$$

correlated the experimental data for a spray. Here, s is the spray penetration, d' is orifice diameter, ρ_a is the density of the air, p is the supply pressure, and t is the time.

C. Spray Cone-Angle and Spray Spreading

The cone angle of a spray is usually defined as the angle between the tangents to the spray envelope at the orifice face. Entrained air has a tendency to reduce the angle slightly at finite distances from the orifice face, but the spray is essentially conical in shape. The cone angle of the spray may also be defined as the angle which includes a specified percentage by weight of the spray, as in Rupe's definition which was noted previously (Ref. 44).

In the present discussion, the cone angle will be taken as the angle enclosing the spray envelope, the term spray spreading will be used to describe the distribution of drops by weight in the enclosed volume of the spray.

Spray dispersion or spreading can be expressed (Ref. 6) by estimating the maximum intensity of the spray, i.e., the maximum volume of fuel collected on unit area of a target transverse to the spray, and expressing the degree of dispersion as the reciprocal of this value. Thus a spray of high intensity is poorly dispersed and the reciprocal of intensity has a small value. Numerical results may have some value in comparing sprays of similar type which are used for the same purpose.

Injection variables usually have opposite effects on cone angle and penetration. Thus, an increase in the density of the surrounding medium, a decrease in fuel viscosity or density, and improved atomization, all tend to increase the spray cone angle.

D. Mean Droplet Size and Droplet-Size Distribution

Droplet size and droplet-size distribution are useful parameters for describing spray characteristics. A description of drop-size distributions was used earlier in this thesis in the discussion of Probert's analysis (Ref. 38).

The fineness of the spray is affected by many variables, such as atomizer design, properties of the liquid and surrounding medium, and discharge velocity. No satisfactory correlation for all these effects on droplet size has as yet been found. Attempts to attack this problem by the use of dimensional analysis will be discussed in Section IV.

The cone angle was found to have little effect on drop size when pressure drops through the nozzle were greater than 30 psi. Below 10 psi, for angles less than 75°, the drop size increased rapidly with decreasing angle. In the low-pressure region, cone angle plays a dominant part in the determination of droplet-size distribution (Ref. 43).

A useful fictitious drop size, which provides a convenient method for comparing two sprays, is the Sauter mean diameter which will be abbreviated to S.M.D. (Ref. 52). The S.M.D. equals the liquid volume of a real spray divided by the surface area of the real spray. It also corresponds to a fictitious spray of uniform droplet size, which has the same liquid volume and the same surface area as the real spray.

Probert's analysis, based on the Rosin-Rammler distribution law (Ref. 38), requires the evaluation of two constants characteristic of the spray. Bevan (Ref. 40) and others (Refs. 41 to 43) indicate that the Rosin-Rammler law applies for many sprays. However, Ingebo (Ref. 13) found that, for his experimental set-up (i.e. simple orifice injector with fuel pressure drop of 55 psi, air velocity 140 to 180 feet per second), the Rosin-Rammler law gave mean droplet diameters which were about one-half of the measured mean droplet diameter; on the other hand, the Nukiyama-Tanasawa (equation 2) and the log-probability methods (equation 4) gave mean drop sizes in good agreement with the size determined by direct integration of the experimental data. The error in mean droplet diameter, computed by using the Rosin-Rammler law, developed because Ingebo chose a number-mean droplet diameter, i.e., the diameter of a drop having an area equal to the ratio of the total surface area of all drops to the total number of drops formed. The Rosin-Rammler expression is of limited use in calculating number-mean droplet diameters since it predicts an infinite number of infinitesimal droplets unless n in equation 1 is greater than 3. Ingebo selected n equal to 3.1. Calculation of a value for n from experimental data in reference 13, using expressions from reference 43, gave a value of n equal to 2.39. The Rosin-Rammler expression has been shown to be of use in computing various mass-mean droplet diameters, i.e., the diameter obtained by giving to each particle diameter a weighting factor proportional to the mass of the particle. Mass means are one of the more important types of averages (Ref. 40). Because of the choice of a number-mean droplet diameter, the failure

of equation 1 to correlate with Ingebo's results does not appear to be important.

Ingebo's experimental results for evaporation rate are well correlated by his theoretical expressions for mass evaporation rate. He states that his data do not agree with the results of Probert's analysis (Ref. 38); the observed discrepancies can probably again be attributed to Ingebo's choice of a number-mean droplet size. He computed S. M. D. from the Nukiyama-Tanasawa expression (equation 2) developed from air-atomizing nozzles while, in his experimental setup, he used a simple orifice pressure atomizer.

As an example of unusual experimental conditions under which equation 1 was found to hold, reference may be made to experiments on liquid wax injected through a fuel nozzle, in which particle size was determined by sieving techniques after solidification of the wax droplets (Ref. 42). Hopkins (Ref. 41) used equation 1 and derived expressions for the weight-mean diameter (the average weight of fuel droplets included in droplets of a particular size range) and the standard deviation of the volume distribution, viz.,

$$d_w = \Gamma\left[\left(1+\frac{1}{n}\right)\bar{D}\right]. \tag{9}$$

In equation 9, d_w is the weight-mean diameter; also

$$\sigma = \bar{D}\sqrt{\Gamma\left[\left(1+\frac{2}{n}\right)\right]-\left[\Gamma\left(1-\frac{1}{n}\right)\right]^2} \tag{10}$$

where σ is the standard deviation and Γ represents, as usual, the gamma function.

Dorsch and Joyce (Ref. 13) analyzed the effects of cone angle, pressure drop, and flow number (F = flow rate in gallons per hour divided by the square root of the pressure drop in psi) on the particle size distribution from a pressure-jet atomizer. They derived expressions for $\bar{D}$ and n based on the flow number (F) of the pressure atomizer and the S.M.D. for the spray. The empirically derived expressions for n, $\bar{D}$, and S.M.D. were developed from log-log plots of S.M.D. versus pressure drops for fixed values of F but variable cone angle. Their results were:

$$\log \bar{D} = (2.7008 + .0261F) - (.3358 - .02427F) \log p, \quad (11)$$

$$\log \text{S.M.D.} = 2.6164 - (.3712 - .02589F) \log p, \quad (12)$$

$$\text{S.M.D.} = \frac{\bar{D}}{\Gamma\left(1-\frac{1}{n}\right)}, \quad (13)$$

where p is the pressure drop in psi.

In actual sprays studied by the wax-particle method, photography, etc., the distribution of droplets by size was found to follow a slightly leptokurtic curve skewed toward the smaller sizes (assuming a distribution from zero to infinity).

E. Effects of Physical Factors of the Fuel and the Surrounding Medium

As the density of the surrounding medium increases, atomization generally improves. It can be assumed that an increase in the temperature of the surrounding medium would have the effect of improving atomization because of increased viscosity, but this is difficult to prove experimentally since the effect of temperature on vaporization rates makes accurate droplet measurements difficult. Since surface tensions and specific gravities of fuels in present use do not vary widely, attention has been directed primarily toward determining the effect of

fuel viscosity on droplet size. The general conclusion is that the fineness of atomization decreases as viscosity is increased.

The effect of an increase in density of the surrounding medium on spray characteristics may be summarized as follows:

(a) the spray velocities decrease, especially at low pressures (i.e., pressures less than 50 psi);

(b) the spray penetration decreases;

(c) the cone angle increases for plain atomizers and decreases for swirl atomizers;

(d) the spray spreading increases;

(e) the mean droplet size decreases.

The effect of the viscosity of the surrounding medium is similar to that of density, but is only appreciable when the flow around the droplets is not turbulent (which is usually not the case).

IV. SIMILITUDE IN SPRAY-NOZZLE PERFORMANCE

Dimensional analysis may be a useful tool for the study of the performance of fuel nozzles. This method of approach helps to define the number of important groups in problems which are too complicated for detailed analytical study. Other investigators (Refs. 6, 45 and 54) have used the methods of dimensional analysis with some success to correlate data on spray-nozzle performance.

The present discussion will be limited to an attempt to obtain the important variables defining mean droplet size for a simple swirl-type nozzle. It is assumed that the mean drop size is defined by the following variables:

d = the mean drop size (dimension ℓ where ℓ denotes length),

ρ_ℓ = the density of the liquid ($m\ell^{-3}$ where m denotes mass),

ρ_m = the density of the surrounding medium ($m\ell^{-3}$),

μ_ℓ = the viscosity of the liquid ($m\ell^{-1}t^{-1}$ where t denotes time),

μ_m = the viscosity of the surrounding medium ($m\ell^{-1}t^{-1}$),

σ_ℓ = the surface tension of the liquid (mt^{-2}),

L = a characteristic length of the nozzle (ℓ),

Δp = the pressure drop across the injection orifice ($m\ell^{-1}t^{-2}$),

θ = the spray angle.

For other types of nozzles additional variables may have to be introduced in order to define the problem. Typical additions might be the following: a length characterizing the swirl chamber dimensions, a fuel pressure in the secondary supply lines for duplex nozzles, a fuel pressure in the return lines for spill-return type nozzles, a length

characterizing the size of the tangential slots, a length characterizing the shape of the orifice, etc.

The following assumptions have been made in listing the nine variables given above for swirl-type nozzles:

(a) Only one length characteristic of the nozzle needs to be introduced. As the result of this, the effects of swirl-chamber design, the shape of tangential slots, orifice construction, etc., are neglected. However, in scaling with maintenance of exact geometric similarity, it is evidently not necessary to consider more than one characteristic length.

(b) Since the temperatures of the liquid and the surrounding medium have not been introduced as important variables, it is assumed that the influence of the temperature can be accounted for fully through the temperature-dependent parameters listed explicitly. The deletion of temperature as an important variable is clearly not justified under conditions where evaporation rates play an important role.

For the nine listed variables expressed in three dimensions, it follows from the Buckingham Pi theorem (Ref. 53) that correlations must involve six dimensionless groups. Following conventional procedures, the following groups were chosen:

$$\frac{d}{L}, \frac{L\Delta p}{\sigma_\ell}, \frac{L(\rho_\ell \Delta p)^{1/2}}{\mu_\ell}, \frac{\rho_\ell}{\rho_m}, \frac{\mu_\ell}{\mu_m},$$

and θ. Here the pressure drop across the injection orifice, Δp, is proportional to $V^2 \rho_\ell$ (V denotes the efflux velocity with the dimensions of ℓt^{-1}); $L\Delta p/\sigma_\ell$ is the Weber number relating inertial to surface tension forces; the group $\frac{L(\rho_\ell \Delta p)^{1/2}}{\mu_\ell}$ is the Reynolds number referred to the characteristic length L. It is now apparent

that d/L should be represented as a function of the other five dimensionless groups if the preceding assumptions are justified. Thus

$$\frac{d}{L} = \phi\left(\frac{L\Delta p}{\sigma_\ell}, \frac{L(\rho_\ell \Delta p)^{1/2}}{\mu_\ell}, \frac{\rho_\ell}{\rho_m}, \frac{\mu_\ell}{\mu_m}, \theta\right). \tag{14}$$

For given fluids the ratios of density and viscosity are constant. In this case, for a given nozzle with fixed spray angle, θ, it follows from equation 14 that the ratio d/L reduces to a function of the Weber and Reynolds numbers only, viz.,

$$\frac{d}{L} = \Phi\left(\frac{L\Delta p}{\sigma_\ell}, \frac{L(\rho_\ell \Delta p)^{1/2}}{\mu_\ell}\right). \tag{15}$$

The validity of equation 15 has been tested by Shafer and Bovey (Ref. 45) using Rupe's experimental data (Ref. 44). Shafer and Bovey found that d/L was a unique function (within $\pm$ 10 %) of Weber number for various Reynolds numbers.

Giffen and Marazew (Ref. 6) have described several applications of dimensional analysis to spray-nozzle performance. Equation 14 has been written in the equivalent form

$$\frac{d}{L} = \psi\left(\frac{V\mu_\ell}{\sigma_\ell}, \frac{LV}{\nu_\ell}, \frac{\mu_m}{\mu_\ell}, \frac{\rho_m}{\rho_\ell}, \theta\right) \tag{16}$$

where the ratio of efflux velocity to the kinematic viscosity, $\frac{V}{\nu_\ell}$ corresponds to $\frac{(\rho_\ell \Delta p)^{1/2}}{\mu_\ell}$ and the Weber number has been replaced by the dimensionless group $\frac{V\mu_\ell}{\sigma_\ell}$ representing Weber number divided by the Reynolds number. For the special case in which the effect of surface tension may be neglected, and the analysis is restricted to a fixed fluid pair, both equations 14 and 16 simplify to

$$\frac{d}{L} = F\left(\frac{Lv}{\nu_\ell}, \theta\right), \tag{17}$$

i.e., the relative droplet size for geometrically similar nozzles is only a function of the Reynolds number and the cone angle.

V. SPRAY EVAPORATION AND ESTIMATES OF THE EVAPORATION CONSTANT (K') FOR VARIOUS SPRAYS

Dahr (Ref. 14) obtained data for evaporation and spreading of an isooctane spray injected counter-current to an airstream. In this work, fuel pressure, air pressure, air velocity, orifice diameter, air temperature, and downstream location of the sampling station were varied. The inlet air temperature had a more marked effect on evaporation than any of the other variables. At first sight it might appear that the degree of atomization had little effect on the percent evaporated. However, it should be noted that pressure drops across the orifice were low and not greatly different for the various runs. Also, the fuel was injected counter-stream and consequently had a relatively long residence time, which would minimize the effects of initial droplet size. Hanson (Ref. 16) found that the evaporation rate was considerably influenced by the relative velocity between the spray and the surrounding airstream. Hanson determined that artificially induced turbulence introduced a lack of uniformity in drop size. Miesse (Ref. 29) studied the ballistics of an evaporating single droplet. Goldsmith (Ref. 32) showed that the gas velocity has no profound effect on evaporation rate.

Ingebo (Ref. 13) studied drop sizes photographically in an experimental setup similar to Bahr's (Ref. 14) and found that, for stations close to the injector, with the counter-stream injection used, all droplets in the duct have the same translational velocity regardless of size (5 - 130 μ). In these tests relative velocities between the droplets and

the airstream were quite high. Reynolds numbers for the large droplets were as high as 400. However, the droplet speed approached the value of airstream velocity within fourteen inches downstream of the injector and was about 80 °/o of airstream velocity five inches downstream of the injector. Use has been made of this last result in the calculations described below.

In order to illustrate how one may use published spray data for estimating effective values of K', some calculations have been carried out using the results of NACA experiments (Refs. 14 and 15) in conjunction with Probert's theoretical curves and empirical expressions for n and $\bar{D}$ in the Rosin-Rammler distribution law (Ref. 43). In reference 14 evaporation data are given for sprays of iso-octane injected counter-stream from a simple orifice injector. Data are reported also (Ref. 15) for evaporation of JP-5 sprays injected counter-stream from a multiple-orifice injector. Experimental data are presented for the percentage evaporated at several sampling stations downstream. Using the tabulated experimental results, the following calculations have been made:

(a) From the fuel-air ratio and the air-flow rate a flow number (F) was obtained.

(b) Using equations 11, 12, and 13, values for $\bar{D}$ and n were calculated. The calculated values are in accord with the data plotted in reference 43.

(c) Using tabulated data (Refs. 14 and 15) for the percentage evaporated and making use of Probert's graph (see figure 1) for the computed values of $\bar{D}$ and n, the parameter $\sqrt{K' t_e}$ was found.

(4) Using the results for $\sqrt{K' t_r}$ at two different downstream sampling positions, and assuming that the droplets traveled with the air velocity, absolute values for K' were computed. The results of these calculations are listed in Tables V and VI.

Examination of the computed evaporation constants, K', shows that they are of the same order of magnitude as the known evaporation constants for one, two, five, and nine droplets burning in air.

REFERENCES

1. Fulton, K. T., "Combustion in the Jet Engine", Aeroplane (March 20, 1953), Vol. 84, No. 2174, pp. 344-348.

2. Graves, C. C., and Gerstein, M., "Some Aspects of the Combustion of Liquid Fuels", Combustion Researches and Reviews, Butterworths Scientific Publications, London (1955), pp. 23-38.

3. Bolt, J. A., and Saxton, M. F., "Fuel Spray Nozzles for Air-Craft Gas Turbines", Automotive Industries (May 15, - June 1, 1949), Vol. 100, No. 10-11.

4. Mock, F. C., and Ganger, D. R., "Practical Conclusions on Gas Turbine Spray Nozzles", S.A.E. Quarterly Transactions (July 1950), Vol. 4, No. 3.

5. McCafferty, R. J., "Effect of Fuels and Fuel Nozzle Characteristics on Performance of an Annular Combustor at Simulated Altitude Conditions", NACA RM E8C02a (Sept. 28, 1949).

6. Giffin, E., and Muraszew, A., The Atomization of Liquid Fuel, John Wiley, New York (1953).

7. Green, J. J., "The Growth of Aeronautical Research in Canada During the Post-War Decade, 11th British Commonwealth and Empire Lecture", Journal of the Royal Aeronautical Society (Dec. 1955), Vol. 59, No. 540, pp. 791-827.

8. Lawrence, O. N., "Fuel Systems for Gas Turbine Engines", Journal of the Royal Aero. Society (Nov. 1955), Vol. 59, No. 539, pp. 727-737.

9. Gerstein, M., "Some Problems Pertinent to the Combustion of Sprays", Combustion Researches and Reviews, Butterworths Scientific Publications, London (1955), pp. 10-22.

10. Sacks, W., "The Rate of Evaporation of a Kerosine Spray", NAE Canada Note 7 (MF2816), Ottawa (1951).

11. Anson, D., "Influence of the Quality of Atomization on the Stability of Combustion of Liquid Fuel Sprays", Fuel (Jan. 1951), Vol. 32, No. 1, pp. 39-51.

12. Wolfhard, H. G., and Parker, W. G., "Evaporation Processes in a Burning Kerosine Spray", Journal of the Institute of Petroleum (Feb. 1949), Vol. 35, No. 302, pp. 118-126.

13. Ingebo, R. D., "Vaporization Rates and Drag Coefficients for Isooctane Sprays in Turbulent Air Streams", NACA TN 3265 (Oct. 1954).

14. Bahr, D. W., "Evaporation and Spreading of Isooctane Sprays in High Velocity Air Streams", NACA RM E53I14 (Nov. 16, 1953).

15. Foster, H. H., and Ingebo, R. D., "Evaporation of JP-5 Fuel Sprays in Airstreams", NACA RM E55K02 (Feb. 21, 1956).

16. Hanson, A. R., "The Evaporation of a Fuel Spray in an Air Stream and the Effect of Turbulence on Droplet Size Distribution", Proceedings of the Second Midwestern Conference on Fluid Mechanics, Ohio State University (Sept. 1952).

17. Godsave, G. A. E., "The Combustion of Drops in a Fuel Spray", NGTE (England), Memorandum No. M. 95 (Oct. 1951).

18. Longwell, J. P., "Combustion of Liquid Fuels", pp. 407-443, Combustion Processes, in Princeton Series on High Speed Aerodynamics and Jet Propulsion, Princeton University Press (1956).

19. Spalding, D. B., Some Fundamentals of Combustion, Butterworth Scientific Publications, London (1955).

20. Spalding, D. B., "Combustion of a Single Droplet and of a Fuel Spray", Selected Combustion Problems, Agard Combustion Colloquium, Butterworths Scientific Publications, London (1954), pp. 340-351.

21. Spalding, D. B., "Combustion of Liquid Fuels", Fourth Symposium (International) on Combustion, Williams and Wilkins, Baltimore (1953), pp. 847-864.

22. Graves, C. C., "Burning Rates of Single Fuel Droplets and Their Application to Turbojet Combustion Processes", NACA RM E53E22 (1953).

23. Browning, J. A., and Krall, W. G., "Effect of Fuel Droplets on Flame Stability, Flame Velocity, and Inflammability Limits", Fifth Symposium (International) on Combustion, Reinhold, New York (1955), pp. 159-163.

24. Ingebo, R. D., "Study of Pressure Effects on Vaporization Rates of Drops in Gas Streams", NACA TN 2850 (Jan. 1950).

25. Kiley, D. W., "On the Burning of Single Drops of Monopropellants", Ae.E. Thesis, California Institute of Technology, Pasadena, Calif. (1955).

26. Ingebo, R. D., "Vaporization Rates and Heat Transfer Coefficients for Pure Liquid Drops", NACA TN 2368 (July 1951).

27. ElWakil, M. M., Uyehara, O. A., and Myer, P. S., "A Theoretical Investigation of the Heating-up Period of Injected Fuel Droplets Vaporizing in Air", NACA TN 3179 (May 1954).

28. ElWakil, M. M., Priem, R. J., Brikowski, H. J., Myers, P. S., and Uyehara, O. A., "Experimental and Calculated Temperature and Mass Histories of Vaporizing Fuel Drops", NACA TN 3490 (Jan. 1956).

29. Miesse, C. C., "Ballistics of an Evaporating Droplet", Jet Propulsion, Journal of American Rocket Society (July - August 1954), Vol. 24, No. 4, pp. 237-244.

30. Rex, J. E., Fuhs, A. E., and Penner, S. S., "Interference Effects During Burning in Air for Two Stationary n-Heptane, Ethyl Alcohol, and Methyl Alcohol Droplets", GALCIT Tech. Report No. 11-1, Contract No. DA 04-495-Ord-446, Pasadena (1955).

31. Goldsmith, M., and Penner, S. S., "On the Burning of Single Drops of Fuel in an Oxidizing Atmosphere", Jet Propulsion (July - August 1954), Vol. 24, No. 4, pp. 245-251.

32. Goldsmith, M., "Experiments on the Burning of Single Drops of Fuel in Air at Various Ambient Conditions", GALCIT Tech. Report No. 9, Contract No. DA-495-Ord-446, Pasadena (May 1955).

33. Fuhs, A. E., "Interference Effects During Burning in Air for Two Stationary Ethyl or Methyl Alcohol Droplets", GALCIT Tech. Report No. 11-2, Contract No. DA-04-495-Ord-446, Pasadena (August 1955).

34. Godsave, G. A. E., "The Burning of Single Drops of Fuel: Part I, Temperature Distribution and Heat Transfer in the Pre-Flame Region", NGTE (England) Report No. R66 (March 1950).

35. Godsave, G. A. E., "The Burning of Single Drops of Fuel: Part II, Experimental Results", NGTE (England) Report No. R87 (April 1951).

36. Wise, H., Lorell, Jack, and Wood, B. J., "The Effects of Chemical and Physical Parameters on the Burning Rate of a Liquid Droplet", Fifth Symposium (International) on Combustion, Reinhold, New York (1955).

37. Hall, A. R., and Diedericksen, J., "An Experimental Study of the Burning of Single Drops of Fuel in Air at Pressures Up to Twenty Atmospheres", Fourth Symposium (International) on Combustion, Williams and Wilkins, Baltimore (1953), pp. 837-846.

38. Probert, R. P., "The Influence of Spray Particle Size and Distribution in the Combustion of Oil Droplets", Philosophical Magazine (Feb. 1946), Vol. 37, No. 265, pp. 94-105.

39. Tanasawa, Y., "On the Combustion Rate of a Group of Fuel Particles Injected Through a Swirl Nozzle, Technology Reports of Tohoku University, Sendai, Japan (1954), Vol. 18, pp. 195-208.

40. Bevans, R. S., "Mathematical Expressions for Drop-Size Distributions in Sprays", Conference on Fuel Sprays, University of Michigan, Ann Arbor, Michigan (March 1949).

41. Hopkins, J. L., "The Size Distribution of Droplets in a Fuel Spray", Tech. Rept. No. ICT/6 Shell Petroleum Co., Ltd., London (Sept. 1946).

42. Joyce, J. R., and Hopkins, J. L., "The Wax Method of Spray Particle Size Measurement", Tech. Rept. No. ICT/7 Shell Petroleum Co., Ltd., London (August 1946).

43. Bowen, I. G., and Joyce, J. R., "The Effects of Cone Angle, Pressure, and Flow Number on the Particle Size of a Pressure Jet Atomizer", Tech. Rept. No. ICT/17 Shell Petroleum Co., Ltd. (March 1948).

44. Rupe, J. H., "A Technique for the Investigation of Spray Characteristics of Constant Flow Nozzles", revised March 1949 to include experimental results, Conference on Fuel Sprays, University of Michigan, Ann Arbor, Michigan (March 1949).

45. Shafer, M. R., and Bovey, H. L., "Applications of Dimensional Analysis to Spray-Nozzle Performance Data", Journal of Research of N.B.S. (March 1954), Vol. 52, No. 3, pp. 141-147.

46. The Penn State Bibliography on Sprays, Second Edition, The Texas Company, New York (1953).

47. Rayleigh, John William Strutt, 3rd Baron, "On the Instability of Jets", Proceedings of London Math. Soc. (England) (1878/1879), Vol. 10, pp. 4-13.

48. Haenlein, A., "Disintegration of a Liquid Jet", NACA Tech. Memo No. 659 (1932).

49. Weber, C., "Züm Zerfalleines Flüssigkeitsstrahles", Zeitschrift für Angewante Mathematik und Mechanik (German)(April 1931), Vol. 11, No. 2, pp. 136-154.

50. Mehlig, H., "Zur Physik der Brennstoffstrahlen in Dieselmaschinen", A.T.Z. (German) (25 August 1934), Vol. 37, No. 16, pp. 411-421.

51. Schweitzer, P. H., "Mechanism of Disintegration of Liquid Jets", Jour. of Appl. Physics (1937), Vol. 8, pp. 513-21. "Spray Penetration", Engg. (England) (1938), Vol. 145, p. 688.

52. Sauter, J., "Determining Size of Drops in Fuel Mixture of Internal Combustion Engines", NACA Tech. Memo No. 390 (1926).

53. Buckingham, E., "On Physically Similar Systems; Illustrations of the Use of Dimensional Equations", Physical Review (1914), Vol. 4, No. 345.

54. Hinze, J. O., "On the Mechanism of Disintegration of High-Speed Liquid Jets", N. V. de Bataafsche Petroleum Mij., Proefstation Delft, Holland, Paper at 6th International Congress on Applied Mathematics, Paris (1946).

TABLE I

EXPERIMENTAL RESULTS FOR THREE-DIMENSIONAL ARRAYS OF NINE n-HEPTANE DROPLETS BURNING IN STILL AIR

RUN	SPACING OF CORNER DROPLETS (mm)	K' (cm^2/sec)	FLAME SHAPE
1-1	9.5	.0119	Separate
2-1	9.5	.0135	Separate
3-1	8.5	.0127	Separate
4-1	8.5	.0119	Separate
1-2	8.5	.0107	Separate
2-2	8.5	.0109	Separate
3-2	8.5	.0123	Separate
4-2	8.5	.0119	Separate
5-2	8.5	.0105	Separate
6-2	8.5	.0109	Separate
7-2	8.5	.0124	Separate
1-3	7.5	.0110	Separate
2-3	7.5	.0114	Separate
5-3	7.5	.0134	Separate
6-3	7.5	.0134	Separate
7-3	7.5	.0128	Separate
8-3	7.5	.0119	Separate
10-3	7.5	.0113	Separate
11-3	7.5	.0107	Separate

TABLE II (Continued)

EXPERIMENTAL RESULTS FOR THREE-DIMENSIONAL

ARRAYS OF NINE n-HEPTANE

DROPLETS BURNING IN STILL AIR

RUN	SPACING OF CORNER DROPLETS (mm)	K' (cm^2/sec)	FLAME SHAPE
6-4	3.6	.0061	Completely Merged
7-4	3.6	.0065	Completely Merged
8-4	3.6	.00775	Completely Merged
10-4	3.6	.0087	Completely Merged
11-4	3.6	.0063	Completely Merged
12-4	3.6	.0085	Completely Merged
13-4	3.6	.00725	Completely Merged
8-5	5.8	.0128	Partially Merged
10-5	5.8	.0129	Partially Merged
11-5	5.8	.0122	Partially Merged
12-5	5.8	.0148	Partially Merged
13-5	5.8	.0126	Partially Merged
14-5	5.8	.0129	Partially Merged
15-5	5.8	.0129	Partially Merged
16-5	5.8	.0127	Partially Merged
17-5	5.8	.0128	Partially Merged
18-5	5.8	.0117	Partially Merged

TABLE II

EXPERIMENTAL RESULTS FOR THREE-DIMENSIONAL ARRAYS OF NINE METHYL ALCOHOL DROPLETS BURNING IN STILL AIR

RUN	SPACING OF CORNER DROPLETS (mm)	K' (cm^2/sec)	FLAME SHAPE
6-1	8.5	.0104	Separate
12-3	7.5	.0110	Separate
13-3	7.5	.0110	Separate
14-3	7.5	.0101	Separate
15-3	7.5	.0120	Separate
16-3	7.5	.0126	Separate
17-3	7.5	.0111	Separate
18-3	7.5	.0097	Separate
1-4	3.6	.00635	Completely Merged
2-4	3.6	.0062	Completely Merged
3-4	3.6	.00545	Completely Merged
4-4	3.6	.00655	Completely Merged
5-4	3.6	.00655	Completely Merged
14-4	3.6	.0066	Completely Merged
15-4	3.6	.0059	Completely Merged
1-5	5.8	.0105	Partially Merged
2-5	5.8	.0106	Partially Merged
3-5	5.8	.0103	Partially Merged
4-5	5.8	.0119	Partially Merged
5-5	5.8	.0104	Partially Merged
6-5	5.8	.0106	Partially Merged
7-5	5.8	.0111	Partially Merged

TABLE III

AVERAGE VALUES OF EVAPORATION CONSTANT (K') FOR NINE-DROPLET ARRAYS OF n-HEPTANE AND METHYL ALCOHOL AS FUELS BURNING IN STILL AIR

FUEL	SPACING OF CORNER DROPLETS (mm)	AVG. K' (cm^2/sec)	NO. OF RUNS	FLAME SHAPE
n-Heptane	9.5	.0127	2	Separate
n-Heptane	8.5	.0116	9	Separate
n-Heptane	7.5	.01225	8	Separate
n-Heptane	5.8	.0128	10	Partially merged
n-Heptane	3.6	.0077	7	Completely merged
Methyl Alcohol	8.5	.0104	1	Separate
Methyl Alcohol	7.5	.0109	7	Separate
Methyl Alcohol	5.8	.0108	7	Partially merged
Methyl Alcohol	3.6	.00637	7	Completely merged

TABLE IV

REPRESENTATIVE VALUES FOR EVAPORATION CONSTANTS FOR ONE, TWO, FIVE, AND NINE n-HEPTANE DROPLETS BURNING IN STILL AIR, DERIVED FROM VARIOUS SOURCES

NO. OF DROPLETS	SOURCE	K' (cm^2/sec)	FLAME SHAPE
1	Ref 31	.0086	
1	Ref 35	.0097	
2	Ref 30	$\cong$ .0080	Merged
2	Ref 30	$\cong$ .0130	Partially merged
2	Ref 30	$\cong$ .0120	Separate
5	Ref 30	.0099	Partially merged
9		.0077	Merged
9		.0128	Partially merged
9		.0119	Separate

TABLE V

RESULTS OF CALCULATIONS OF K' FOR ISOOCTANE SPRAYS INJECTED COUNTER-STREAM, BASED ON DATA GIVEN IN REFERENCE 14.

((Fuel pressure drop = 55 psi, orifice diameter = .041 inches, air pressure = 25 inches Hg, Flow number (F) = 2.29, S.M.D. = 118 microns, $\bar{D}$ = 183 microns, n (Distribution constant in Rosin - Rammler law) = 2.35)).

AIR TEMPERATURE ($^{\circ}R$)	AIR VELOCITY (ft/sec)	DISTANCE DOWNSTREAM FROM INJECTOR (in)	$\sqrt{K' t_r}$ (cm x 10^{-4})	K' ($cm^2/sec \times 10^{-3}$)
545	147	5.25	59	
				8.27
545	147	10.4	82.5	
545	147	5.25	59	
				9.24
545	147	18.25	102	
545	147	10.4	82.5	
				10
545	147	18.25	102	
545	197	5.25	66	
				12.4
545	197	10.4	82.5	
545	197	5.25	66	
				11.1
545	197	18.25	106	

TABLE V (cont'd)

RESULTS OF CALCULATIONS OF K' FOR ISOOCTANE SPRAYS INJECTED COUNTER-STREAM, BASED ON DATA GIVEN IN REFERENCE 14.

((Fuel pressure drop = 55 psi, orifice diameter = .041 inches, air pressure = 25 inches Hg, Flow number (F) = 2.29, S.M.D. = 118 microns, $\bar{D}$ = 183 microns, n (Distribution constant in Rosin - Rammler law) = 2.35)).

AIR TEMPERATURE (^{o}R)	AIR VELOCITY (ft/sec)	DISTANCE DOWNSTREAM FROM INJECTOR (in)	$\sqrt{K' t_r}$ (cm x 10^{-4})	K' ($cm^2/sec \times 10^{-3}$)
690	228	10.4	119	
				16
690	228	18.25	132	
690	270	10.4	123	
				22
690	270	18.25	143	
790	193	5.25	139	
				14.4
790	193	10.4	150	
780	240	5.25	150	
				41.4
780	240	10.4	172	

TABLE VI

RESULTS OF CALCULATIONS OF K' FOR JP-5 SPRAYS INJECTED COUNTER-STREAM, BASED ON DATA GIVEN IN REFERENCE 15.

((Fuel pressure drop = 26 psi, multiple-orifice injector, air pressure = 25 inches Hg, Flow number (F) = 2.69, S.M.D. = 155 microns, $\bar{D}$ = 230 microns, n (Distribution constant in Rosin-Rammler law) = 2.35)).

AIR TEMPERATURE ($^{\circ}$R)	AIR VELOCITY (ft/sec)	K' ($cm^2/sec \times 10^{-3}$)
760	216	1.75 - 2.80
760	270	1.68 - 1.88
760	324	2.62 - 1.20
760	370	1.70 - 2.64
960	216	0.69 - 1.50
960	270	1.23 - 2.63
960	324	2.80 - 1.20
960	370	4.7 -11.3
1160	216	6.16 - 3.6
1160	270	8.8 - 8.95
1160	324	
1160	370	27.0 -41.0

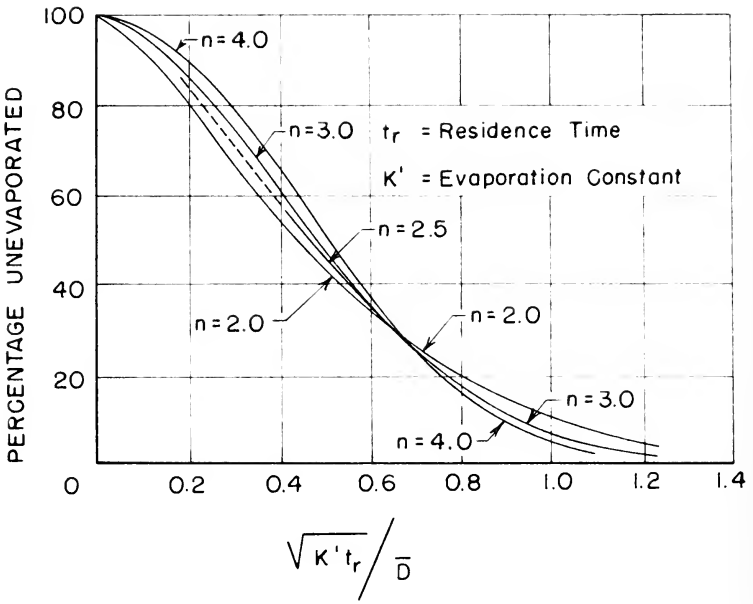

FIG. 1 – PERCENTAGE OF UNEVAPORATED (UNBURNT) FUEL AS A FUNCTION OF $\sqrt{K' t_r}/\overline{D}$ AND n FOR SPRAYS OBEYING THE ROSIN-RAMMLER DISTRIBUTION LAW (AFTER PROBERT, REF. 38)

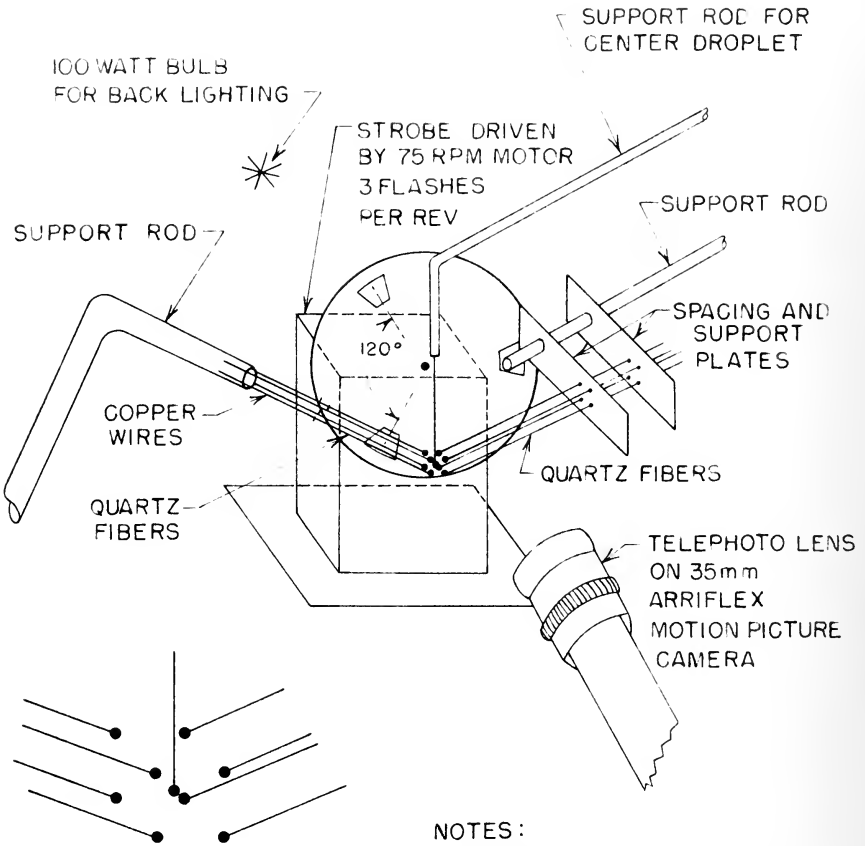

DETAIL OF FIBER ARRANGEMENT

NOTES:

1. DISTANCE FROM CAMERA LENS TO CENTER DROPLET ≈5".
2. ALL SUPPORT RODS CLAMPED TO PORTABLE STANDS FOR POSITIONING.
3. DISTANCE OF BULB FROM DROPLETS ≈7".

FIG. 2 – SCHEMATIC ARRANGEMENT OF APPARATUS FOR PHOTOGRAPHING NINE-DROPLET ARRAYS

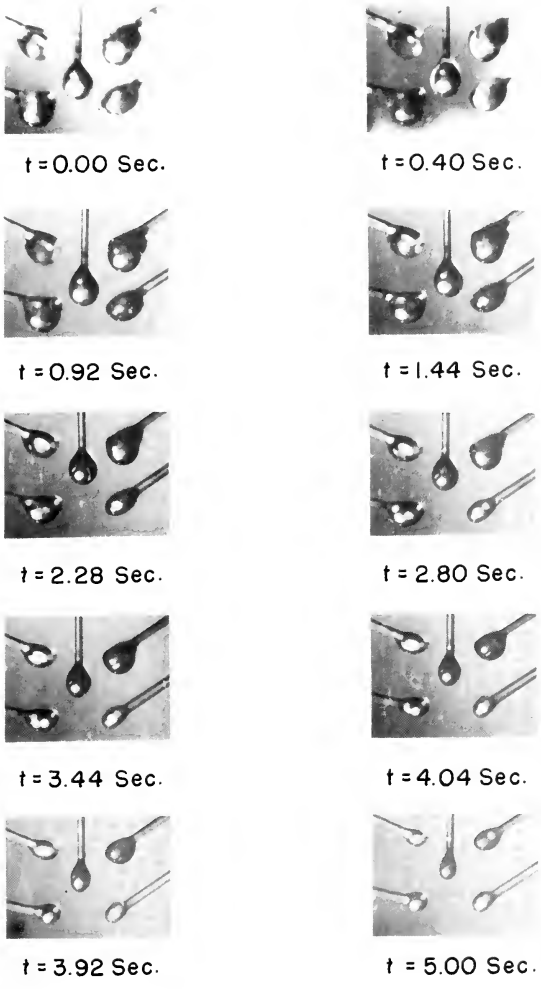

FIG. 3 – PHOTOGRAPHS OF ONE RUN FOR BODY-CENTERED CUBIC SPATIAL ARRANGEMENT OF NINE METHYL ALCOHOL DROPLETS BURNING IN AIR. CUBE EDGE SPACING OF 3.6mm; K' FOR CENTER DROPLET = 0.0063 $cm.^2/sec.$

Cube Size 7.5 mm (Edge Measurement). Separated Flame Envelopes For Each Droplet. Average $K' = 0.0109$ cm^2/sec.

Cube Size 5.8 mm. Partially Merged Flame Envelopes. Average $K' = 0.0108$ cm^2/sec.

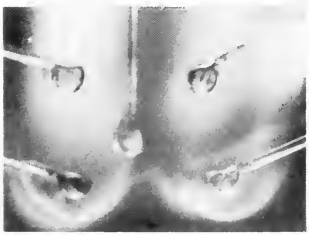

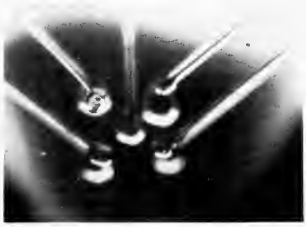

Cube Size 3.6 mm. Completely Merged Flame Envelopes. Average $K' = 0.00637$ cm^2/sec.

FIG. 4 – PHOTOGRAPHS OF FLAME SHAPES OBSERVED FOR BODY-CENTERED CUBIC SPATIAL ARRANGEMENT OF NINE n-HEPTANE DROPLETS BURNING IN AIR FOR VARYING CUBE SIZES

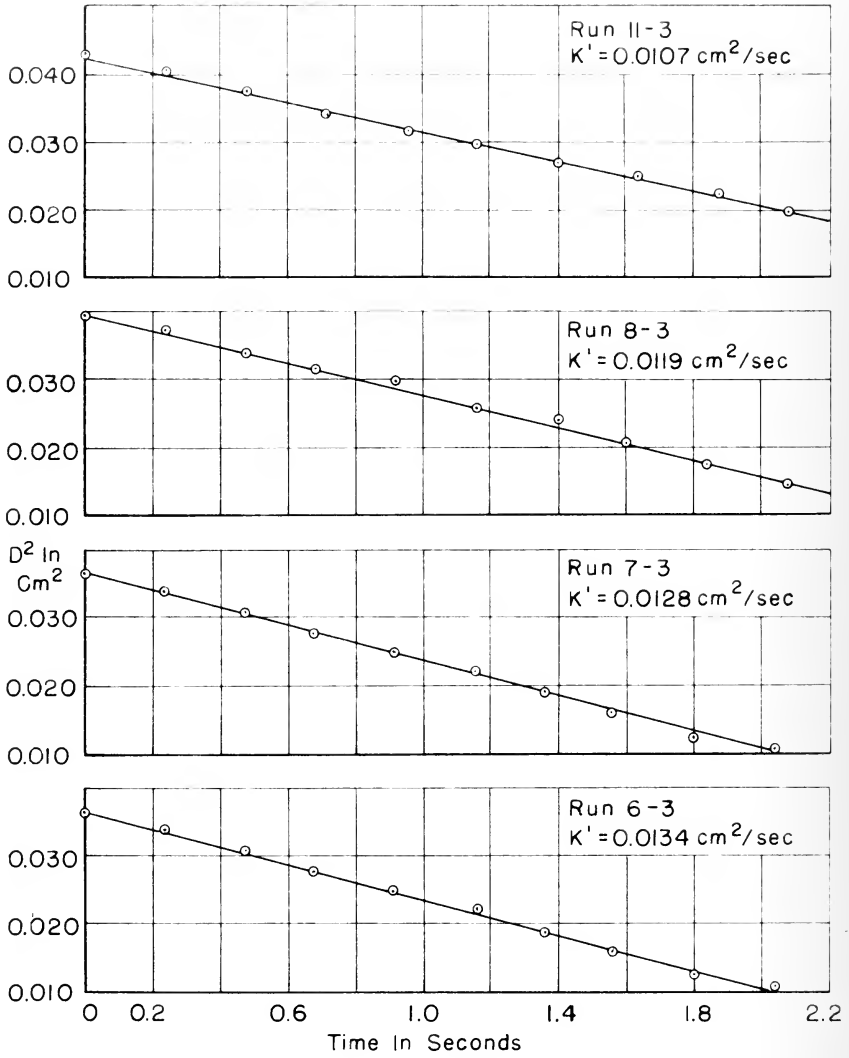

FIG. 5 – VARIATION OF D^2 WITH TIME FOR CENTER DROPLET IN NINE DROPLET THREE-DIMENSIONAL ARRAY WITH *n*-HEPTANE AS FUEL AND CUBE EDGE SPACING OF 7.5 mm.

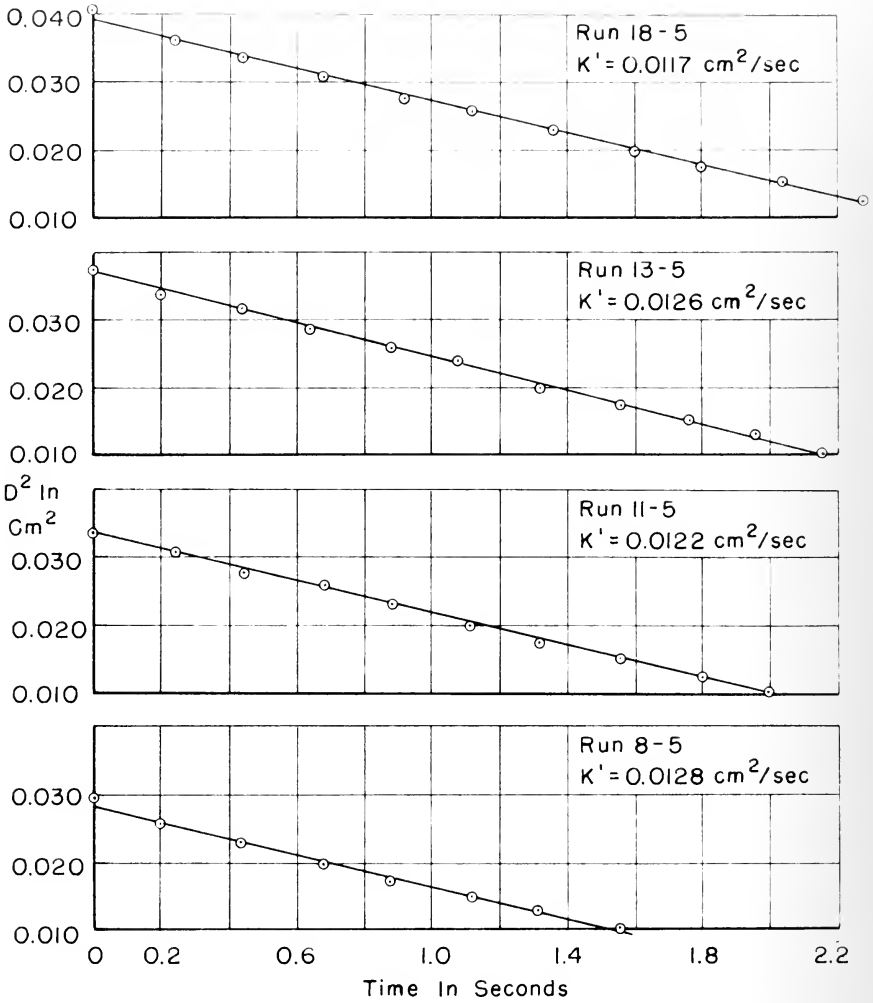

FIG. 6 - VARIATION OF D^2 WITH TIME FOR CENTER DROPLET IN NINE DROPLET THREE-DIMENSIONAL ARRAY WITH n-HEPTANE AS FUEL AND CUBE EDGE SPACING OF 5.8 mm.

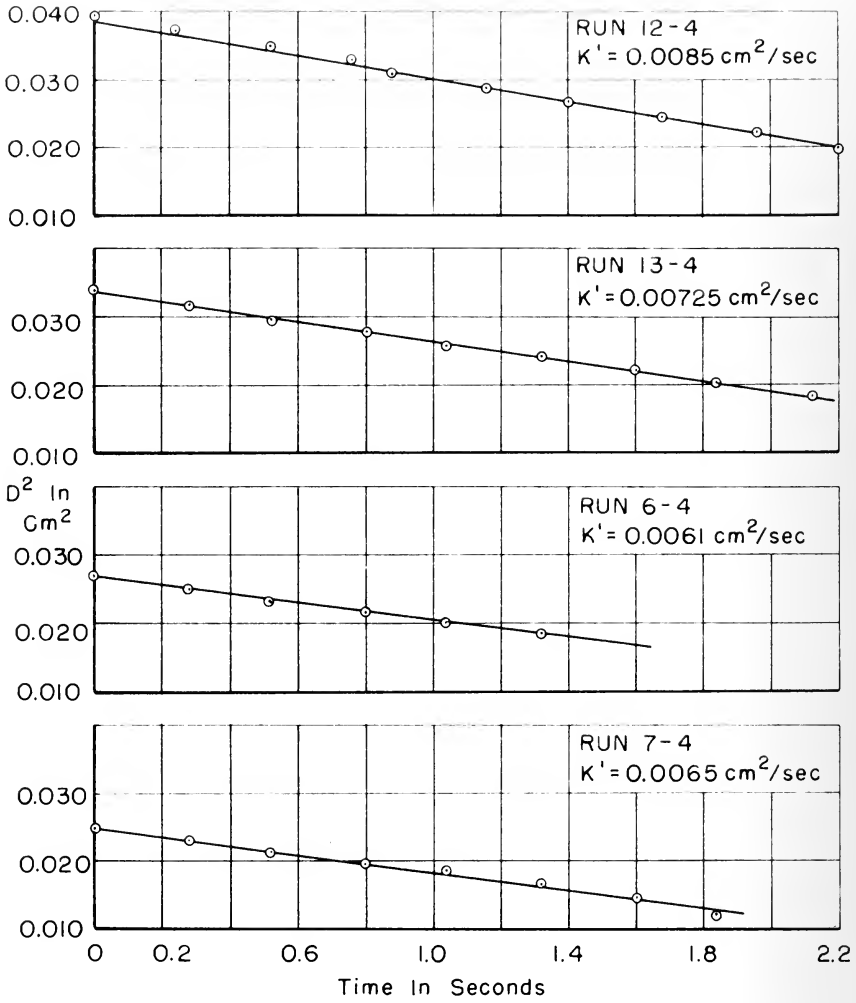

FIG. 7 - VARIATION OF D^2 WITH TIME FOR CENTER DROPLET IN NINE DROPLET THREE-DIMENSIONAL ARRAY WITH n-HEPTANE AS FUEL AND CUBE EDGE SPACING OF 3.6 mm.

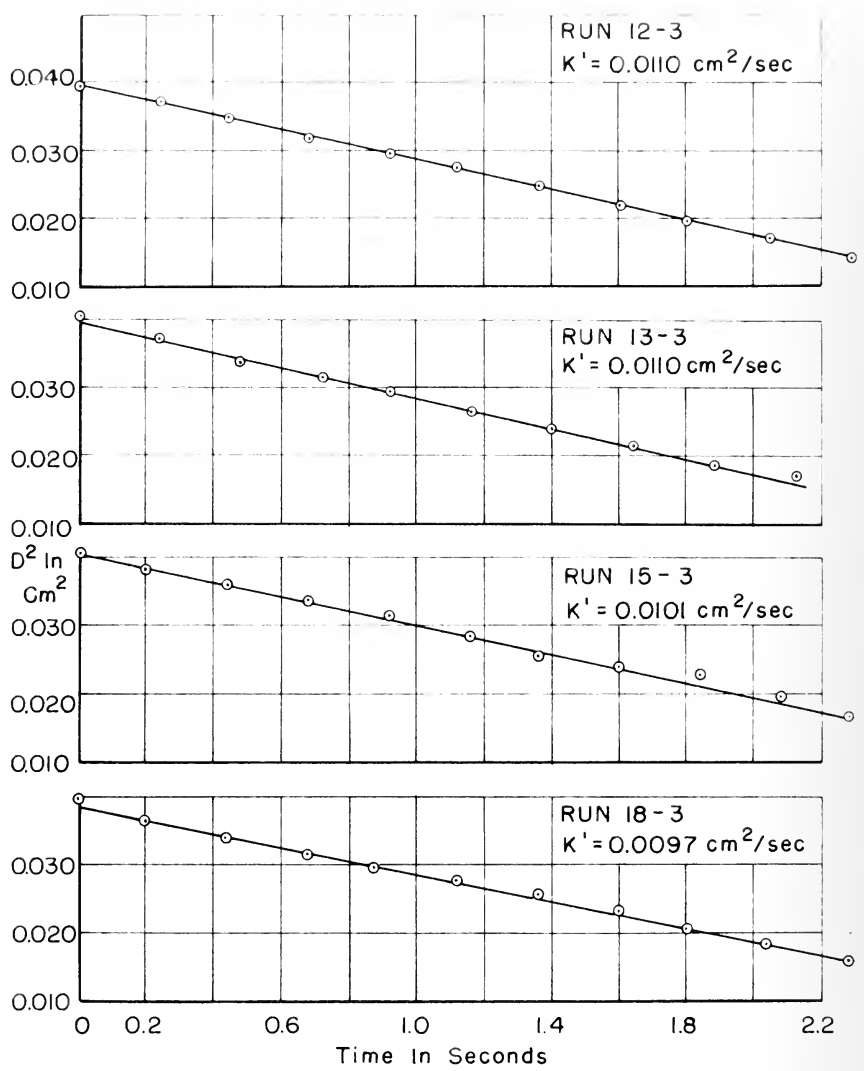

FIG. 8 – VARIATION OF D^2 WITH TIME FOR CENTER DROPLET IN NINE DROPLET THREE-DIMENSIONAL ARRAY WITH METHYL ALCOHOL AS FUEL AND CUBE EDGE SPACING OF 7.5 mm.

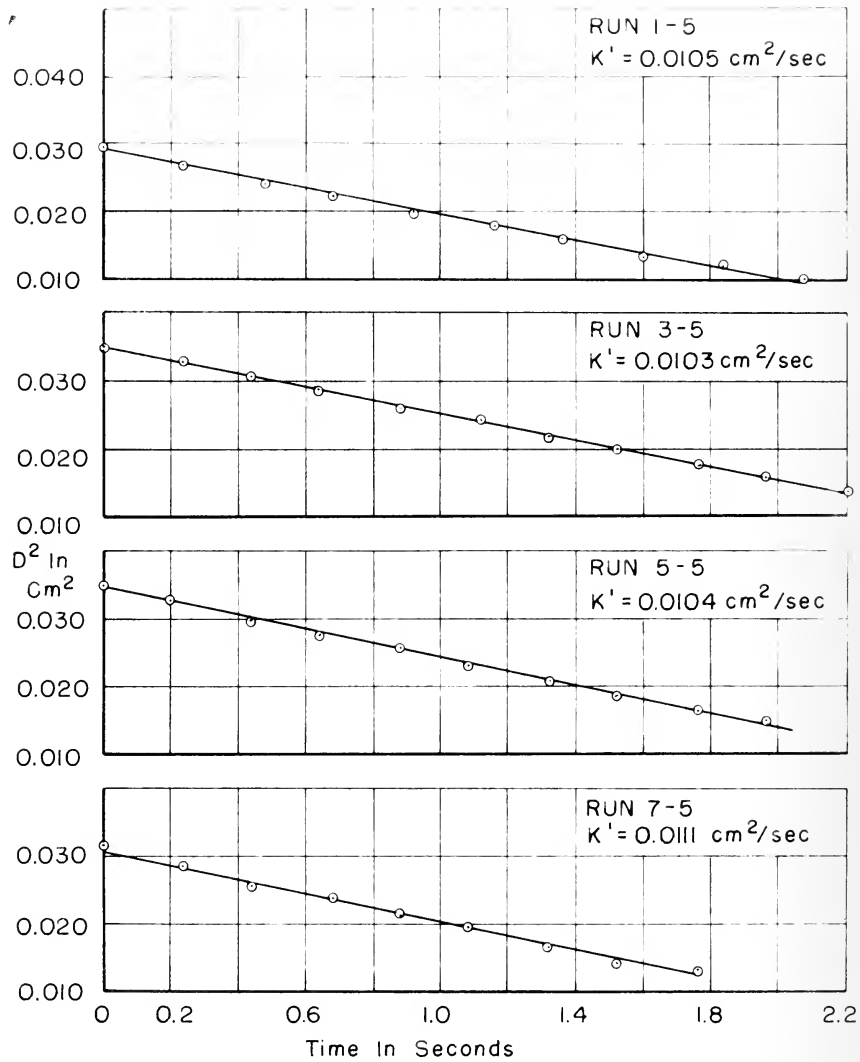

FIG. 9-VARIATION OF D^2 WITH TIME FOR CENTER DROPLET IN NINE DROPLET THREE-DIMENSIONAL ARRAY WITH METHYL ALCOHOL AS FUEL AND CUBE EDGE SPACING OF 5.8 mm.

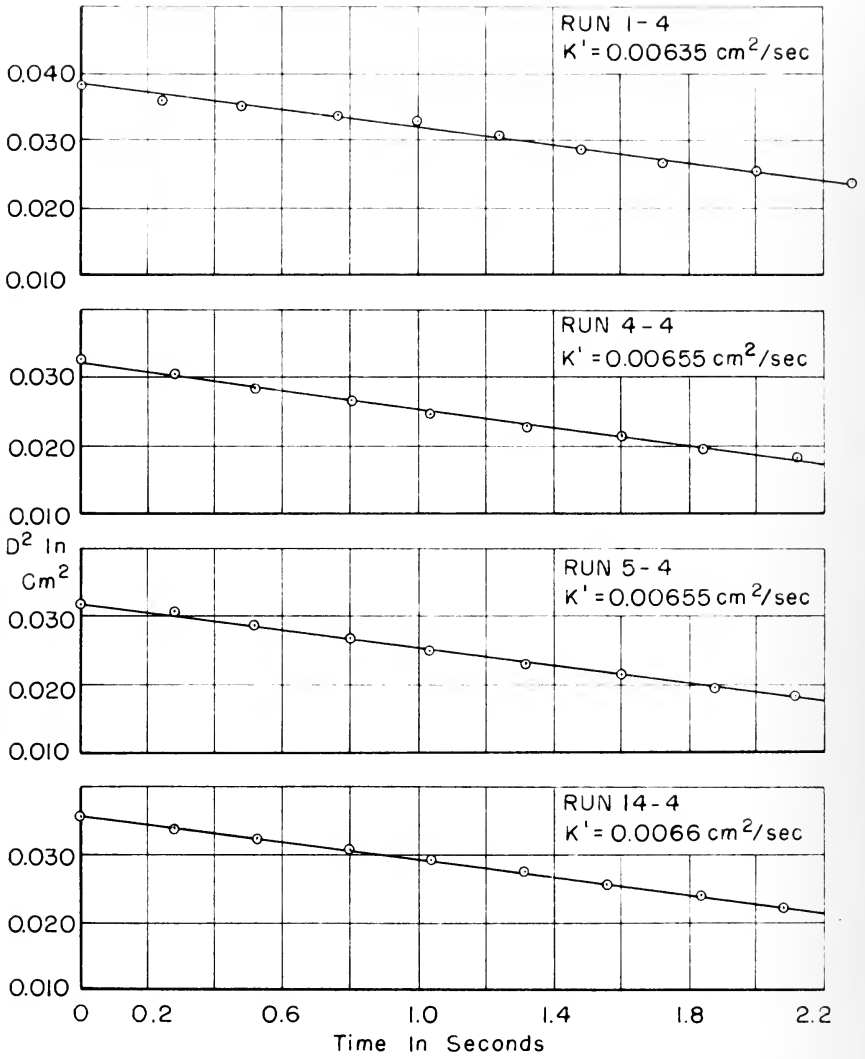

FIG. 10 – VARIATION OF D^2 WITH TIME FOR CENTER DROPLET IN NINE DROPLET THREE-DIMENSIONAL ARRAY WITH METHYL ALCOHOL AS FUEL AND CUBE EDGE SPACING OF 3.6 mm.

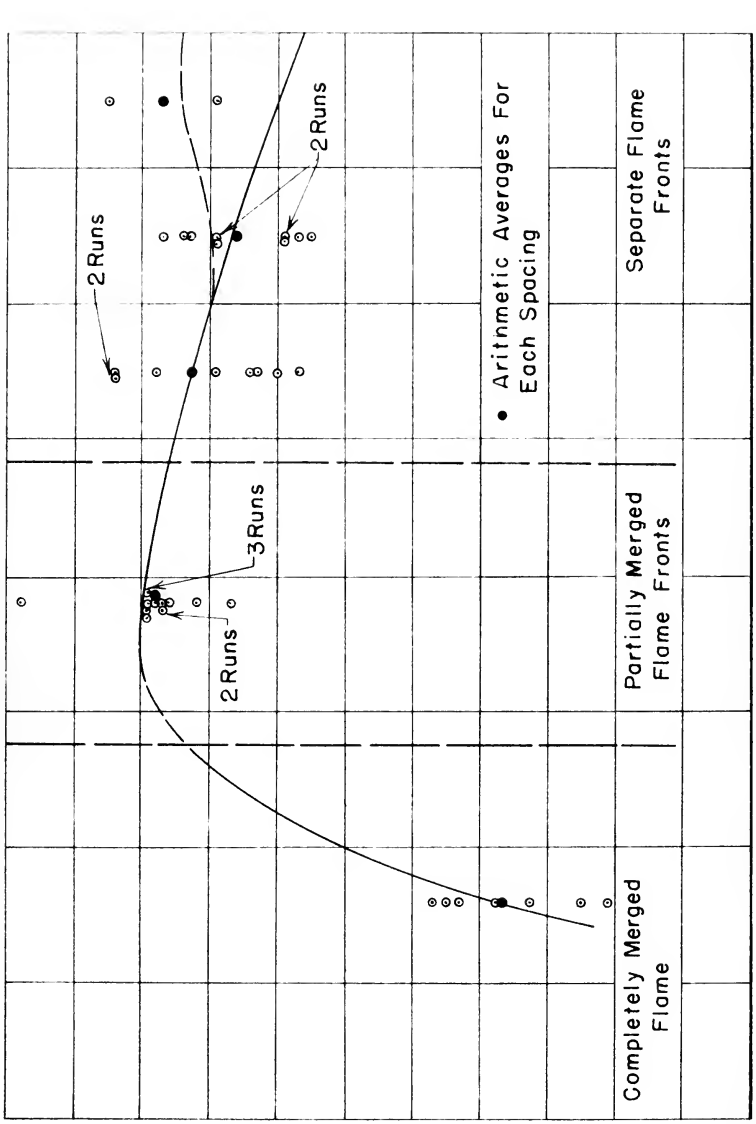

FIG. 11 - EVAPORATION CONSTANT (K') vs. CUBE SPACING FOR CENTER DROPLET OF NINE-DROPLET ARRAY WITH n - HEPTANE AS FUEL

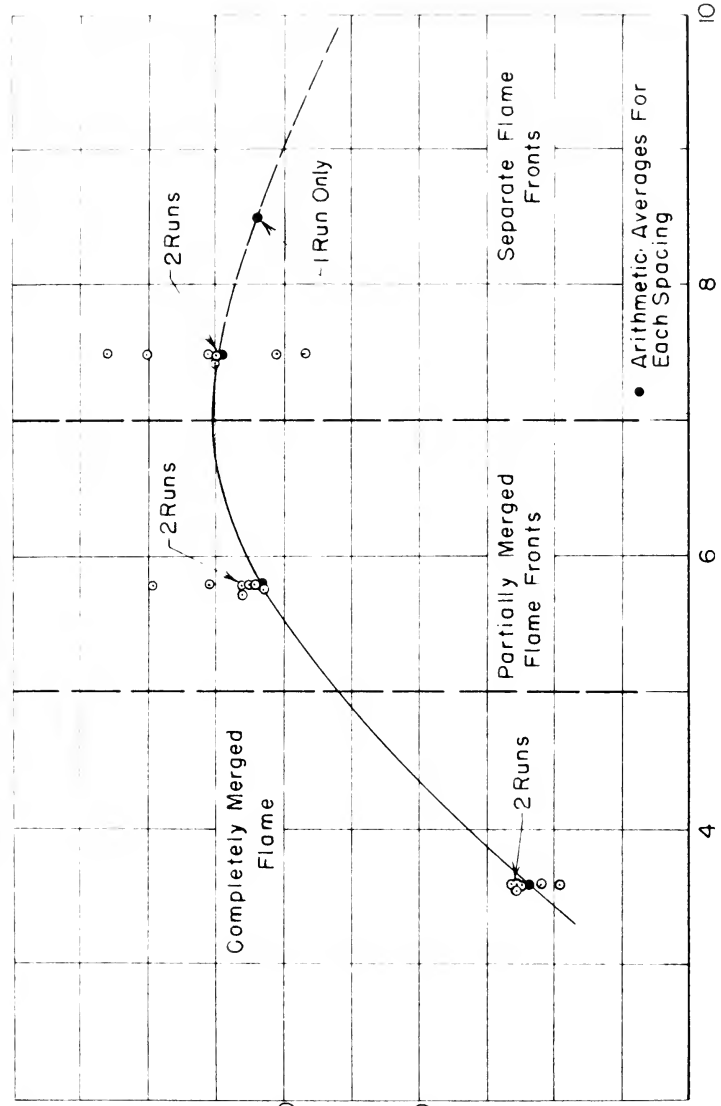

FIG. 12 - EVAPORATION CONSTANT (K') vs. CUBE SPACING FOR CENTER DROPLET OF NINE-DROPLET ARRAY WITH METHYL ALCOHOL AS FUEL

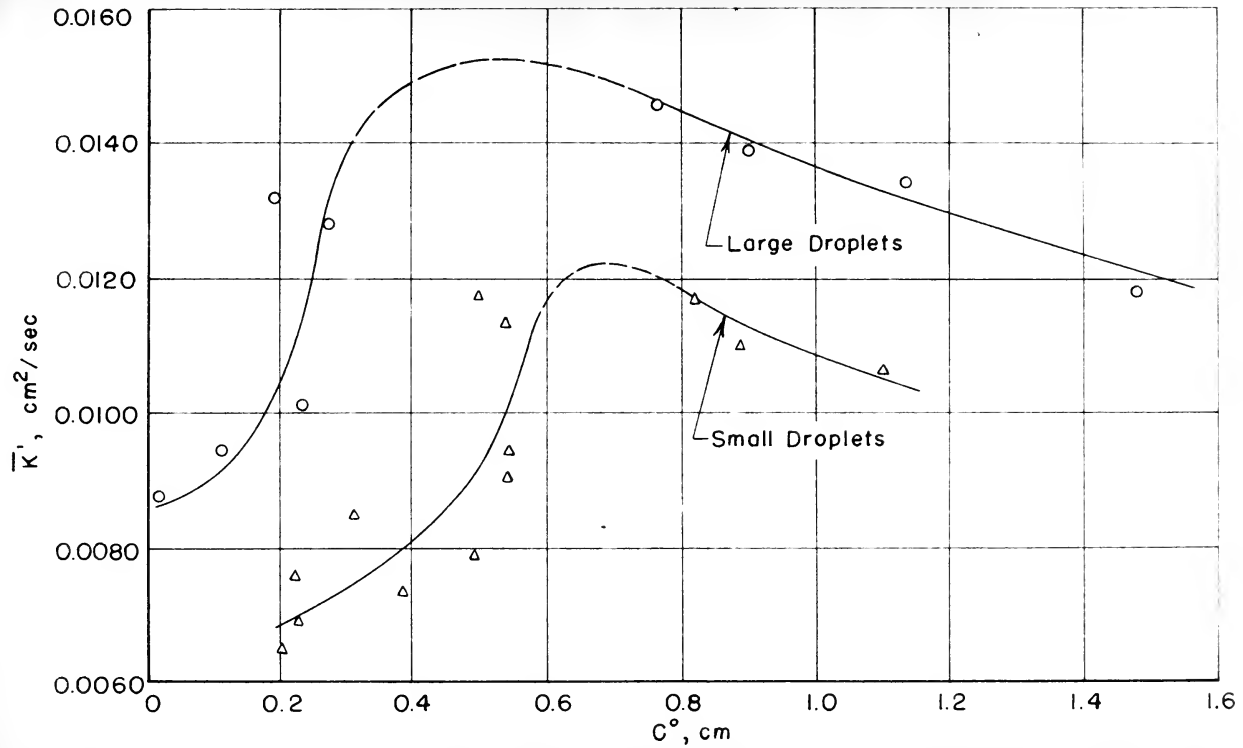

FIG.13- VARIATION OF THE AVERAGE EVAPORATION CONSTANT WITH SPACING FOR TWO n-HEPTANE DROPLETS WITH DIFFERENT INITIAL AVERAGE DIAMETERS $\overline{D}°$(FROM REF. 30)